Calibration of Nonlinear Variable Loads Based on Manifold Learning

Alejandro J. Venere, Martin Hurtado, and Carlos H. Muravchik
Research Institute of Electronics, Control and Signal Processing - LEICI
National University of La plata (UNLP), La Plata, Argentina
Email: alejandro.venere@ing.unlp.edu.ar

***Abstract*—In this work, we present a method for calibrating non-linear variable impedances based on the manifold-learning technique. This approach circumvents the dependency on the analytical model of the device, and works under the assumption that the impedance values come from a "black box" controlled by a number of independent parameters. The goal of the calibration is to recover the unknown control parameters that set the load into the desired impedance states. We tested the proposed procedure first on a simulated example and then on the prototype presented in [1] at a frequency of 1575.42 MHz. The results based on both simulated and real data showed accurate recovery of the control parameters.**

***Index Terms*—diffusion map, manifold learning, variable loads.**

I. Introduction

Variable impedances are used in many modern systems operating at microwave frequencies. For instance, they have been applied for the automatization of measuring noise in two-port devices [2], for tuning wireless systems [3], and for different parts of communication systems including electronically controlled attenuators [4] and modulators [5], phase shifters [6], reconfigurable antennas [7], and six-port modulators [8]. In all these examples, the variable impedance operates as an adaptive device to provide a circuit with a tunable adjustment or matching. Depending on their design, most of the variable impedances are controlled through several nonlinear parameters. Then, a calibration process is required in order to recover the unknown parameter values which set the desired impedance states.

In [2], the control parameters are estimated from the synthesis formulas of the specific load circuit. However, this approach requires a precise model of the device. Most of the time, a detailed model is not available because of the effect of parasitic components at high frequency and the lack of accurate characterization provided by the manufacturer. Herein, we propose a general procedure for calibrating any variable impedance based on the manifold learning method known as diffusion map. Instead of exploiting the predefined model of the circuits, this method provides an intrinsic modeling from a reparametrization of the load. Diffusion map was applied by Coifman and Lafon for dimensionality reduction in many fields [9], and recently, it was showed to be also useful for modeling systems whose responses are a nonlinear function of several independent parameters [10].

In this work, we propose a calibration approach based on manifold learning that does not require the model of the load. It is a data-driven method that relies on measurements of the load values to build an affinity matrix. The principal component analysis applied to this matrix generates the reparametrization. Nevertheless, the new parameters are not exactly the true parameters of the load, but they are related through a monotonic transformation. Therefore, the calibration procedure consists of the following stages. First, we process training data to compute the optimal diffusion kernel which represents the concept of affinity among the observed impedance values and captures the features of the nonlinear behavior of the load. Then, the eigen-decomposition of the affinity matrix leads to the inverse mapping from the observations to the parameters. Finally, we interpolate points in the reparametrized space to generate the parameters of new impedance states. Herein, the described procedure is used for calibrating a variable load at a single frequency. We tested the proposed method to calibrate the load presented in [1] which is a complex-valued impedance controlled by two current sources. We employed the method on both, synthetic and real data collected from the prototype of this impedance at a frequency of 1575.42 MHz. Both synthetic and real results showed accurate recovery of control parameters.

II. Problem formulation

When a transmission line with characteristic impedance Z_0 is loaded with an impedance Z, their mismatch is represented by the reflection coefficient

$$\Gamma = \frac{V^-}{V^+} = \frac{Z - Z_0}{Z + Z_0} \in \mathbb{C}. \tag{1}$$

The reflection coefficient is the ratio between the backward wave V^- generated at the load and the forward wave V^+ impinging on the load. In several microwave systems, it is required to control the complex amplitude V^-. For example, in a six-port modulator [8], variable loads are used to generate different reflection coefficients on the respective ports of the six-port network, which in turn modulate an applied carrier signal.

Herein, we address the calibration of the variable impedance presented in [1] operating at a frequency of 1575.42 MHz. It is a termination load that consists of a Wilkinson power divider connecting two pin diodes through transmission lines

of different electric lengths. Each diode is polarized by means of a bias current causing a (nonlinear) change of its resistance. Then, the complex value of the reflection coefficient is set through a combination of two variables, the pin diode bias currents. Although the relationship between the input V^+ and the output V^- is linear with respect to the impedance, we remark that the value of the impedance is nonlinear with respect to the two controlling currents; and so is the reflection coefficient.

Throughout this paper, we use the following notation. Let $\bar{\Gamma} = \left\{\bar{\gamma}^i\right\}_{i=1}^m$ be a set of m observations of the reflection coefficient generated by the variable impedance when the controlling parameters are $\bar{\Theta} = \left\{\bar{\theta}^i\right\}_{i=1}^m$. Each parameter $\bar{\theta}^i$ is a $d \times 1$ vector. In addition, the set $\left\{\theta^{i_j}\right\}_{j=1}^L$ denotes additional parameters corresponding to L small perturbations of $\bar{\theta}^i$. The reflection coefficients generated by these additional parameters are shaped like a "point cloud" around the observation $\bar{\gamma}^i$. We assume the set $\bar{\Gamma}$ and the corresponding point clouds consist of the training data available beforehand. Moreover, let $\Gamma = \left\{\gamma^i\right\}_{i=1}^M$ be the set of M desired reflection coefficients and $\Theta = \left\{\theta^i\right\}_{i=1}^M$ be the set of corresponding control parameters. The goal of the calibration is to recover the unavailable set of control parameters in Θ from Γ.

III. Calibration method

This section describes the calibration method that is constructed from the diffusion map algorithm proposed by Coifman and Singer in [10]. At first, the behavior of the training observations is picked up building the diffusion kernel. Then, its eigen-decomposition leads to an inverse mapping from the observations to the parametric (current values) space. The fit of the kernel is then optimized iteratively. We divide the method in three parts: the computation of the diffusion kernel; the eigen-decomposition of the kernel matrix; and the computation of the optimal kernel parameter. A summary of the implementation of the calibration method is presented at the end of this section.

A. Diffusion kernel

Following [10], the kernel is computed from a secund-order approximation of the Euclidean distance between parameters, given by

$$\| \theta^i - \theta^j \|^2 \approx 2(\gamma^i - \gamma^j)^T \left[C_{\gamma^i}^{-1} + C_{\gamma^j}^{-1}\right](\gamma^i - \gamma^j) \quad (2)$$

where C_{γ^i} is the covariance which represents the distortion around the observation γ^i due to small perturbations of θ^i. The additional information of the local distortion is available from perturbations of the corresponding control parameters in $\bar{\Theta}$. Then, we are able to empirically estimate the covariance matrix for only the training observations in $\bar{\Gamma}$ with

$$C_{\bar{\gamma}^i} = \frac{1}{L}\sum_{j=1}^{L}(\bar{\gamma}^{i_j} - \mu_i)(\bar{\gamma}^{i_j} - \mu_i)^T \quad (3)$$

where $\mu_i = \frac{1}{L}\sum_{j=1}^{L}\bar{\gamma}^{i_j}$, and $\left\{\bar{\gamma}^{i_j}\right\}_{j=1}^L$ is the point cloud around $\bar{\gamma}^i$ given by the set of parameters $\left\{\theta^{i_j}\right\}$.

We build the $M \times m$ affinity matrix A between observations in $\bar{\gamma}$ and the desired values γ. The affinity is based on the Gaussian kernel with scale parameter ε as follows

$$A_{ji} = exp\left\{-\frac{\| C_{\bar{\gamma}^i}^{-1}(\bar{\gamma}^i - \gamma^j) \|^2}{\varepsilon}\right\} \quad (4)$$

where the index j and i denote the row and the column of the matrix A, respectively. From matrix A we compute the $m \times m$ kernel matrix W which represents the affinity among training observations in $\bar{\Gamma}$, and is given by

$$W = S^{-\frac{1}{2}} A^T A S^{-\frac{1}{2}} \quad (5)$$

where S is a diagonal matrix containing the sum of $A^T A$ along rows. Alternatively, W can be also be computed as

$$W_{ji} = \frac{\pi}{\sqrt{\det(C_{\tilde{\gamma}})}} \times \exp\left\{-\frac{(\bar{\gamma}^i - \bar{\gamma}^j)^T\left[C_{\bar{\gamma}^i}^{-1} + C_{\bar{\gamma}^j}^{-1}\right](\bar{\gamma}^i - \bar{\gamma}^j)}{\varepsilon}\right\} \quad (6)$$

where $\tilde{\gamma} = \left(\bar{\gamma}^i + \bar{\gamma}^j\right)/2$.

B. Kernel eigen-decomposition

From the normalized matrix $\tilde{A} = AS^{-\frac{1}{2}}$ we compute its singular values decomposition. Let $\{\lambda_i\}_{i=1}^m$, $\{\varphi_i\}_{i=1}^m$, and $\{\psi_i\}_{i=1}^M$ be the singular values and the left and right singular vectors of $\tilde{A}$, respectively. Note that $\left\{\lambda_i^2\right\}$ and $\{\varphi_i\}$ are the eigenvalues and eigenvectors of the matrix (5), and establish the reparametrization of the observations in $\bar{\Gamma}$. Then, the embedding of $\bar{\Gamma}$ into the parametric space formed by the eigenvectors of W is given by

$$\Phi_d : \bar{\gamma}^i \rightarrow \left[\lambda_1^2\varphi_1(\bar{\gamma}^i), ..., \lambda_d^2\varphi_d(\bar{\gamma}^i)\right]^T. \quad (7)$$

The dimension of the space, d, is established by taking the d eigenvectors corresponding to the largest eigenvalues. By the same token, $\{\psi_i\}$ are the eigenvectors of $\tilde{A}\tilde{A}^T$ and establish the reparametrization of desired values of Γ. They can be calculated from φ_i as follows

$$\psi_i = \frac{1}{\lambda_i}\tilde{A}\varphi_i. \quad (8)$$

The mapping function from observations in Γ to the reparametrization space formed by d eigenvectors denoted in descending order, is

$$\Psi_d : \gamma^i \rightarrow \left[\psi_1(\gamma^i), ..., \psi_d(\gamma^i)\right]^T. \quad (9)$$

In order to obtain the unavailable control parameters in Θ we compute the following weighted sum of training parameters in $\bar{\Theta}$

$$\hat{\theta}^i = \sum\nolimits_{j:\Psi(\bar{\gamma}^i)\in\mathcal{N}_i} \rho_j(\gamma^i)\bar{\theta}^j \quad (10)$$

where $\mathcal{N}_i$ consists of k-nearest neighbors of $\Psi(\gamma^i)$ in the training samples, and $\rho_j(\gamma^i)$ are the linear interpolation coefficients which result from solving the linear system given by

$$\left\{\bar{\theta}^j\right\}_{j:\Psi(\bar{\gamma}^i)\in\mathcal{N}_i} = \left\{\rho_j(\gamma^i)\Psi_d\left\{\bar{\gamma}^j\right\}\right\}_{j:\Psi(\bar{\gamma}^i)\in\mathcal{N}_i}. \quad (11)$$

In [10] a different interpolation between points in Ψ_d is proposed. We applied the calibration method in the simulated example presented in Sec. IV, computing (11) for both interpolation alternatives. By using the linear interpolation, the method recovered the controlling parameters with more accuracy.

C. Scale parameter

The scale parameter ε is a measure of similarity between points in the observation space. The computation of the affinity matrix (4) and the performance of the algorithm are sensitive to its value. In order to find the optimal value of the scale parameter, we define a validation error which will be minimized as function of ε.

First, in [10] is defined Φ^{-1} as the inverse mapping from the available parameters to the observable space, which approximates the training observations in $\bar{\Gamma}$

$$\Phi^{-1}(\bar{\theta}) = \sum\nolimits_{i:\bar{\theta}^i \in \mathcal{B}_\theta} \beta_i(\bar{\theta})\bar{\gamma}^i \tag{12}$$

where $\mathcal{B}_\theta$ is a set of the neighbors of $\bar{\theta}$, and β_i are interpolation coefficients given by

$$\beta_i(\bar{\theta}) = \frac{\exp\left(\frac{-\|\bar{\theta}-\bar{\theta}^i\|^2}{\sigma_{\beta_i}}\right)}{\sum_{i:\bar{\theta}^i \in \mathcal{B}_\theta} \exp\left(\frac{-\|\bar{\theta}-\bar{\theta}^i\|^2}{\sigma_{\beta_i}}\right)} \tag{13}$$

where σ_{β_i} denotes the minimal distance between $\bar{\theta}^i$ and its nearest neighbor. Then, the validation error is defined as follows

$$E_V(\bar{\gamma}^i) = \|\bar{\gamma}^i - \Phi^{-1}(\bar{\theta}^i)\|^2, \tag{14}$$

and measures the accuracy of the function Φ^{-1} in estimating $\bar{\gamma}^i$. We compute the mean validation error by averaging (14) for all training observations. Then, we use a procedure to obtain the optimal value of the scale, which minimizes the mean error. The said procedure is represented by the training stage in the following section.

D. Implementation of the method

The proposed calibration method is employed in two stages: first, a training stage based on the optimization of the Gaussian kernel scale ε; second, an estimation stage where the unknown control parameters in Θ are recovered.

==========

Training stage:

1) Obtain m observations corresponding to the training samples of the controlling parameters $\bar{\Theta}$
2) Given clouds of the additional observations corresponding to perturbations of the training parameters, compute the local covariance C of each training observation by (3).
3) Compute the Kernel matrix W from (6), by using an arbitrary kernel scale ε.
4) Employ the eigenvalues decomposition of W and obtain the eigenvalues $\{\lambda_i^2\}$ and eigenvectors $\{\varphi_i\}$.
5) Construct the map Φ_d according to (7) from the eigenvalues and eigenvectors of W.
6) Construct the inverse map Φ_d^{-1} from (12).
7) Repeat 3 - 6 for different scale ε, and find the optimal value that minimizes the mean validation error (14).

==========

Estimation stage:

1) Given all the desired values Γ, compute the normalized affinity matrix $\tilde{A}$ according to (4) using the optimal value of ε.
2) Calculate ψ_i as a weighted combination of φ_i via (8).
3) Construct the map Ψ_d according to (9), to obtain the reparametrization of the controlling parameters.
4) Recovered the unknown control parameters via (10).

IV. Simulated Example

Following the description of the variable impedance in [1], we built a model to synthesize observations of the impedance of the load as function of the bias currents, which are the control parameters. By sweeping both current values in the range of [0,40] mA we obtain the coverage area of the impedance, which is mapped on the Smith chart by normalizing the values through the characteristic impedance $Z_0 = 50\Omega$, as shown in Fig. 1. Worthwhile to mention that the model is a simplification of the real response of the load because its parameters are considered constant and independent of the frequency and the bias currents. Such assumptions are not true in practice.

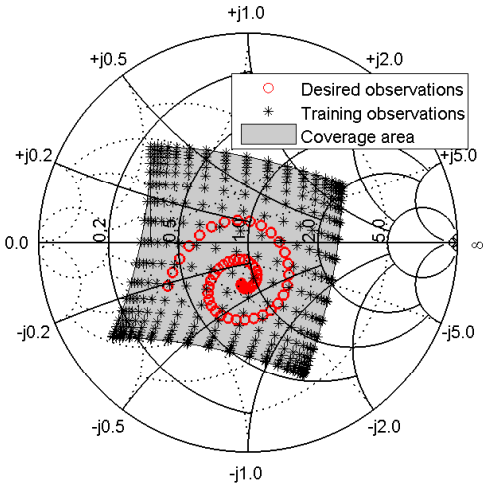

Fig. 1. Simulated response of the variable impedance [1] mapped on the Smith chart. Coverage area along with training observations $\bar{\Gamma}$ and desired observations in Γ

In order to calibrate this simulated device, we selected the training parameters $\bar{\Theta}$ to generate the observations $\bar{\Gamma}$ as follows: both currents were swept in the range of [0,40] mA, taking 20 logarithmically spaced values per current source. The combination of the current values produce $m = 400$ training impedance values. In addition, the desired values are selected to form a spiral in the Smith chart. Fig. 1 shows the desired and the training reflection coefficients in the

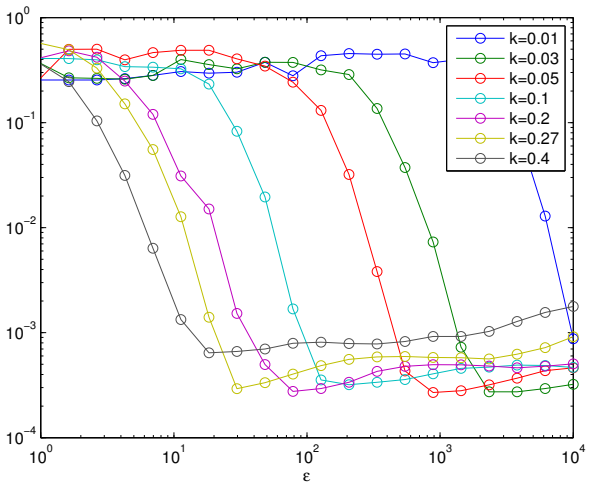

Fig. 2. Mean validation error obtained from training observations as function of the scale ε, from different values of the variance constant k.

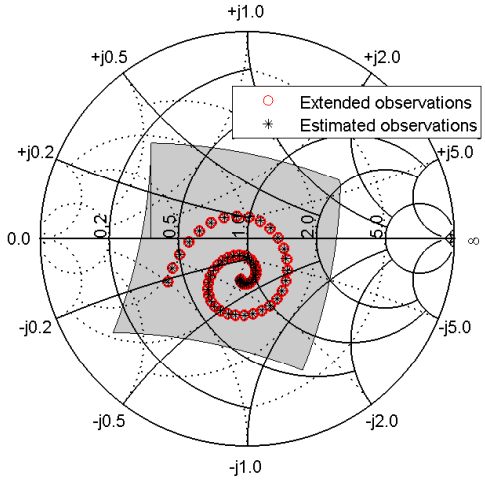

Fig. 3. Simulated response of the variable impedance [1] mapped on the Smith chart. Desired observations compared with estimated observations.

Smith chart computed by (1) with the characteristic impedance $Z_0 = 50\Omega$.

Following on the method, each training parameter in $\bar{\Theta}$ is used to generate the additional parameters $\{\theta^{i_j}\}$ obtaining the clouds around the observations in $\bar{\Gamma}$. Specifically, we generated $L = 20$ Gaussian distributed values around the current values $\{\bar{\theta}_1^i\}$ and $\{\bar{\theta}_2^i\}$ in the following way

$$\theta_1^{i_j} = \bar{\theta}_1^i + n_j(\bar{\theta}_1^i) \quad (15)$$

$$\theta_2^{i_j} = \bar{\theta}_2^i + n_j(\bar{\theta}_2^i) \quad (16)$$

where $n_j(\bar{\theta}^i) \sim \mathcal{N}(0, \bar{\theta}^i k)$ is a random variable and $k \in \mathbb{R}$ is a constant. By using both sets $\left\{\theta_1^{i_j}\right\}_{j=1}^{L}$ and $\left\{\theta_2^{i_j}\right\}_{j=1}^{L}$ we produce the point cloud around the observation $\bar{\gamma}^i$. Note that the variance of the Gaussian distribution of $n_j(\bar{\theta}^i)$ depends on the value of $\bar{\theta}^i$, in this way, we aim that the clouds around training observations present similar sizes. Thus, the non-linearity between the parameters and the observations around the entire coverage area is explored.

We follow the steps of the training stage of the method by using training observations in $\bar{\Gamma}$ and the corresponding point clouds. By repeating steps 2 for different constants k and 3 for different scale values, we obtain the mean validation error (14) by averaging over all training observations as function of k and ε, as shown in Fig. 2. We stress the following points: when increasing the value of k, the minimal value of the mean validation error appears on a smaller scale ε, and viceversa. On the other hand, for values of k larger than 0.27, the minimal error value begins to get worse. Thus, we choose an intermediate value of $k = 0.05$, which obtains the minimum error, on the scale $\varepsilon = 1000$ approximately. Now, we are able to compute the estimation stage, where the control currents of the desired impedance states are recovered. Thus, from the normalized matrix $\tilde{A}$, computed with the optimal parameter values of k and ε, we construct the mapping function Ψ_2 by (8). In order to obtain the unavailable control parameters in Θ, we compute (10). Finally, we use the recovered control currents $\hat{\theta}$ into the simulated model of the load to obtain an estimate of the desired reflection coefficients. To quantify the accuracy of the method, we defined the following estimation error

$$E_M = \frac{1}{M}\sum_{i=1}^{M}\frac{\|\gamma_e^i - \gamma^i\|}{\|\gamma^i\|} \quad (17)$$

where γ_e is the estimated value of the desired reflection coefficient γ. In this case, the estimation error (17) results $E_M = 0.038\%$, exhibiting great match between the points in the Smith chart, as shown in Fig. 3.

V. Measured Example

Herein we consider the prototype of the variable impedance [1] implemented at 1575.42 MHz. This prototype is an impedance termination controlled by two digital current sources whose values can vary between $[0, 40]$ mA with a resolution of $\Delta I = 9.76$ μA. To establish the impedance states of the load, a computer controls the current sources transmitting 12-bit words through a serial peripheral interface. Then, the digital words generate quantized values of the currents, which are the controlling parameters. In this work, the estimated parameters in (10) take any value between $[0, 40]$ mA because the parameters in (9) does not include information about the quantized values of the currents, and this issue will be reflected in the estimation error of the results. We used the method for calibrating the prototype by taking the same training parameters $\bar{\Theta}$ defined in the simulated example. Each training parameter $\bar{\theta}^i$ is used to generate $L = 20$ perturbations computed by (17) with $k = 0.05$. Therefore, we measured the impedance response to these current values and obtained the 400 training observations and the corresponding point clouds. Then, we considered the set of desired impedance values, which forms a spiral in the Smith chart. Fig. 4 shows the

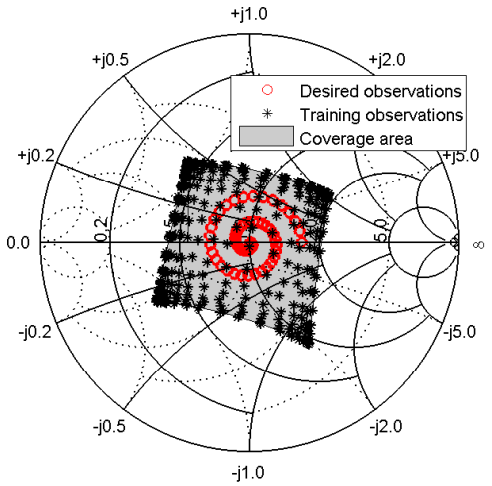

Fig. 4. Measured response of the variable impedance [1] at 1575.42 MHz. Coverage area along with training observations $\bar{\Gamma}$ and desired observations in Γ.

training reflection coefficients of the prototype along with the desired spiral in the Smith chart, all computed with a characteristic impedance $Z_0 = 50\Omega$.

Once all training data are measured, we repeat the steps $3-7$ of the training stage for different values of the scale ε, and we find the optimal value of the scale corresponding to the minimum value of the mean validation error. Fig. 5 shows the mean validation error as function of the scale ε. The optimal value of ε results near to 1000.

Finally, we compute the estimation stage and obtain the mapping Ψ_2. We found the unavailable control currents from (10) and measured the response of the prototype to these values. The estimation error (17) results $E_M = 7\%$. The estimated and the desired observations are shown in Fig. 6.

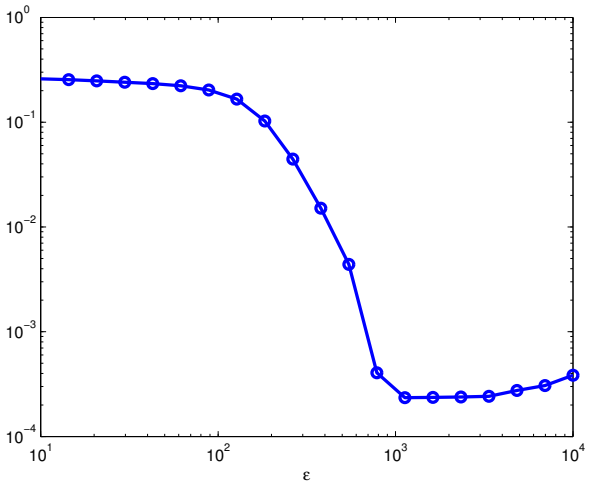

Fig. 5. Mean validation error as a function of the scale ε of the Gaussian kernel computed for all training data of the prototype

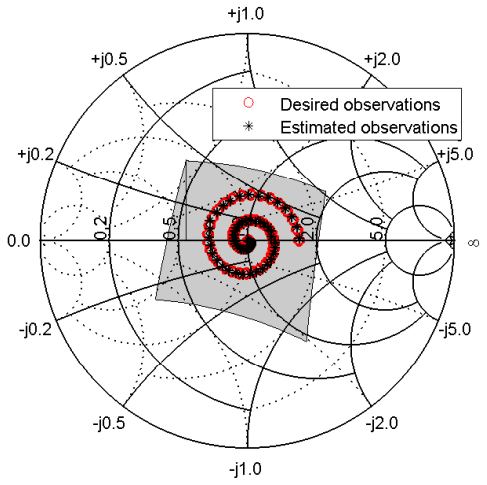

Fig. 6. Measured response of the variable impedance [1] at 1575.42 MHz. Desired observations compared with estimated observations.

These results show great match among points in the Smith chart.

VI. Conclusion

In this work, a method for calibrating non-linear variable impedances based on the manifold-learning technique was proposed. This calibration approach, instead of exploiting the analytical model of the device whose parameters are somewhat uncertain, , is based on a supervised algorithm that learns the intrinsic model of the load through a set of training data. Based on the assumption that variable impedances are controlled by several independent parameters, the goal of the method is the recovery of those control parameters to establish a set of desired impedance values at the operating frequency. We utilized the method on both synthetic and real data. The latter was a prototype of the variable load presented in [1] that consists of a complex-valued impedance controlled by two current sources polarizing two pin diodes in ports of a Wilkinson divider. For both examples, we showed that the calibration method can accurately recover the desired control currents of the load, even in the practical example that results difficult modeling the response of the load.

For future research, we plan to extend the calibration procedure to the frequency domain. We aim to determine the controlling bias current that set the variable load to produce a desired impedance at different operating frequencies. Therefore, the training data must include observations of the reflection coefficients at different frequencies.

VII. Acknowledgment

This work was supported by the ANPCyT under Grant PICT-2014-1232, the National University of La Plata under Grant I-209, and the CIC - PBA.

REFERENCES

[1] A. J. Venere, M. Hurtado, R. L. La Valle, and C. H. Muravchik, "New Design of a Variable Impedance Based on Polarized Diodes at Microwave Frequency," *IEEE Microwave and Wireless Components Letters*, vol. 27, no. 5, pp. 470–472, May 2017.

[2] B. M. Albinsson, H. Guo, M. Schoon, and H. O. Vickes, "A new programmable load for noise parameter determination," *IEEE Transactions on Microwave Theory and Techniques*, vol. 39, no. 2, pp. 216–223, Feb. 1991.

[3] T. Pochiraju, V. F. Fusco, J. Francey, and H. Schmassmann, "Low-power variable impedance load/tuning unit," *Electronics Letters*, vol. 44, no. 21, pp. 1258–1259, Oct. 2008.

[4] K.-O. Sun, M. K. Choi, and D. v. d. Weide, "A PIN diode controlled variable attenuator using a 0-dB branch-line coupler," *IEEE Microwave and Wireless Components Letters*, vol. 15, no. 6, pp. 440–442, Jun. 2005.

[5] J. K. Hunton and A. G. Ryals, "Microwave Variable Attenuators and Modulators Using PIN Diodes," *IRE Transactions on Microwave Theory and Techniques*, vol. 10, no. 4, pp. 262–273, Jul. 1962.

[6] M. Tsuji, T. Nishikawa, K. Wakino, and T. Kitazawa, "Bi-directionally fed phased-array antenna downsized with variable impedance phase shifter for ISM band," *IEEE Transactions on Microwave Theory and Techniques*, vol. 54, no. 7, pp. 2962–2969, Jul. 2006.

[7] C. Gu, S. Gao, H. Liu, Q. Luo, T. H. Loh, M. Sobhy, J. Li, G. Wei, J. Xu, F. Qin, B. Sanz-Izquierdo, and R. A. Abd-Alhameed, "Compact Smart Antenna With Electronic Beam-Switching and Reconfigurable Polarizations," *IEEE Transactions on Antennas and Propagation*, vol. 63, no. 12, pp. 5325–5333, Dec. 2015.

[8] Y. Zhao, C. Viereck, J. F. Frigon, R. G. Bosisio, and K. Wu, "Direct quadrature phase shift keying modulator using six-port technology," *Electronics Letters*, vol. 41, no. 21, pp. 1180–1181, Oct. 2005.

[9] R. R. Coifman and S. Lafon, "Diffusion maps," *Applied and Computational Harmonic Analysis*, vol. 21, no. 1, pp. 5–30, Jul. 2006. [Online]. Available: http://www.sciencedirect.com/science/article/pii/S1063520306000546

[10] R. Talmon, D. Kushnir, R. R. Coifman, I. Cohen, and S. Gannot, "Parametrization of Linear Systems Using Diffusion Kernels," *IEEE Transactions on Signal Processing*, vol. 60, no. 3, pp. 1159–1173, Mar. 2012.